ISSN 1991- 8690
الترقيم الدولي 8690 - 1991
website :http://jsci.utq.edu.iq
Email:utjsci@utq.edu.iq

Electrochemical, thermodynamic and quantum chemical studies of thoron compound as new corrosion inhibitor for C-steel in Acidic Media

Munther Abdul-Jaleel Mohammed-Ali* Alaa Ali Husain** Ekhlas Qanber Jasim*

* Pharmaceutical Chemistry Department- College of Pharmacy- Basrah University-Basrah, Iraq
** Chemistry Department - College of Education for Pure Sciences - Basrah University- Basrah, Iraq
*E-mail: muntheralamery@yahoo.com

Abstract

The corrosion rates in the presence of thoron as a steel corrosion inhibitor in 1M HCl and 1M H_2SO_4, were measured by the weight loss method, potentiodynamic polarization measurements and quantum chemical calculations. The weight loss method was studied in different times (1-4 hr) and in the range of temperatures from 298 to 318 K. Results obtained revealed that thoron performed excellently as a corrosion inhibitor for C-steel in these acids media and its efficiency attains to 91.99% at $1x10^{-3}$M at 298 K, and by potentiodynamic polarization measurements its efficiency attains to 93.74% in the same conditions. The Langmuir adsorption isotherm was tested for their fit to the experimental data. The apparent activation energies, enthalpies and entropies of the dissolution process and the free energies and equilibrium constants for the adsorption process were determined and discussed. All the computed quantum chemical parameters are found to correlate well with experimental inhibition efficiencies of inhibitor.

Keyword: corrosion, azo dye, thermodynamic, quantum chemistry.

دراسة الكتروكيميائية وثرموديناميكية وكيمياء الكم لمركب الثورون كمثبط تآكل جديد للفولاذ الكاربوني في اوساط حامضية

منذر عبدالجليل محمدعلي* الاء علي حسين** اخلاص قنبر جاسم*

* فرع الكيمياء الصيدلانية – كلية الصيدلة – جامعة البصرة
** قسم الكيمياء – كلية التربية للعلوم الصرفة– جامعة البصرة

الخلاصة

تم قياس سرعة التآكل بوجود مركب الثورون كمثبط للتاكل للفولاذ الكاربوني في وسطين 1مولاري من كل من حامض الهيدروكلوريك وحامض الكبريتيك باستخدام طريقة الفقدان بالوزن وقياسات جهد الاستقطاب وحسابات كيمياء الكم. درست طريقة الفقدان بالوزن في ازمان (1–

4 ساعات) ضمن مدى حراري 298– 318 كلفن. اشارت النتائج ان لمركب الثورون فعالية تثبيط ممتازة للفولاذ الكاربوني في هذه الوساط الحامضية حيث وصلت كفاءة التثبيط الى 91,99% بتركيز $1x10^{-3}$ مولاري وحرارة 298 كلفن. اما باستخدام قياسات جهد الاستقطاب فقد وصلت الكفاءة الى 93,74%. كما لوحظ ايضا، ان امتزاز الجزيئات على سطح المعدن يخضع لمعادلة امتزاز لانكماير. تم تعيين قيم الثوابت الثرموديناميكية، طاقة التنشيط وحرارة التفاعل والعشوائية لعملية ذوبان السبيكة وتم كذلك تعيين الطاقة الحرة وثوابت الاتزان لعملية الامتزاز، وتم مناقشة هذه النتائج. وجد هناك تناسق كبير بين القيم العملية لكفاءة التثبيط والقيم المحسوبة من كيمياء الكم.

1. Introduction

Mild steel in acid solution is widely used in various industrial processes and corrosion of mild steel known to occur in this environment [1,2]. One of the effective methods to prevent corrosion is the use of organic inhibitors [3]. Organic inhibitors were adsorbed on a metallic surface. Water molecules at metallic surface are replaced by organic inhibitor molecules. In case of chemisorption, the formation of a bond between the metal and organic inhibitor impedes the anodic and cathodic processes, thereby protecting the metal surface [3]. Furthermore, inhibitor adsorption is influenced by factors such as the nature and surface charges on the metal, type of aggressive media, structure of inhibitor, and the nature of its interaction with the metal surface. The effective organic inhibitors contain nitrogen, sulfur and oxygen atoms. Moreover, sulfur containing compounds are preferred for H_2SO_4 while those containing nitrogen act more effectively in HCl [4].

Azo compounds have attracted considerable attention due to their impressive and useful chemical and physical properties [5,6]. Apart from their purely chemical interest, azo ligands have also received special attention because of their mixed soft–hard donor characters (O, N and S donor sites), versatile coordination behavior [7,8], pharmacological properties [9,10] and optical and thermal properties [11].

The aim of the present work is to study the inhibitive action of azo dye compound (thoron) toward the corrosion inhibitor of carbon-steel in 1M HCl and 1M H_2SO_4 solutions using weight loss and galvanostatic polarization techniques. The effect of temperature on the dissolution of carbon-steel in free and acidic solutions was also investigated, and some thermodynamic parameters for activation process were computed.

2. Experimental part

2.1. Materials

Hydrochloric acid, sulfuric acid and acetone were obtained from Aldrich Chemicals. The mono azo dye compound (thoron, o-arsono-phenylazo-2-naphthol-3,6-disulfonic acid sodium salt) used as inhibitor was obtained from Merck with the purity better than 98.5% and has the following structure:-

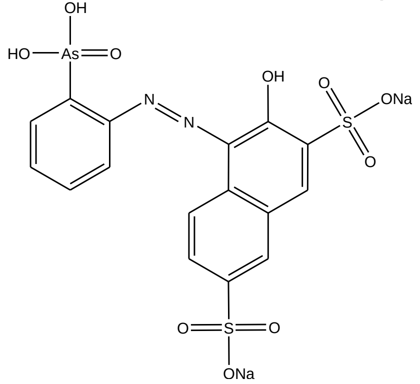

Thoron structure

2.2. Solutions preparation

The aggressive solutions 1M HCl and 1M H_2SO_4, were prepared by dilution of analytical grade 37% HCl and 98% H_2SO_4 with distilled water, respectively. The tested inhibitor (thoron) was prepared in different concentration $1x10^{-5}$, $1x10^{-4}$ and $1x10^{-3}$ in the previous acidic solutions.

2.3. Weight loss method

Inhibitor efficiency was determined at 298, 308 and 318 k for 1, 2, 3 and 4 h by immersing vertically the steel coupon of dimensions 3.5 cm 2.5 cm 0.4cm into acid solutions (100 cm^3) containing various concentrations of inhibitor.

After the elapsed time, the coupons were cleaned through a procedure that consisted of wiping the coupons with a paper tissue, washing with distilled water, acetone followed by oven drying at 110^{o}C.

2.4. Electrochemical measurements

Polarization studies were carried out using Bank EIEIKTRONKIK INTELLGENT CONTROLS Model MLab 200-ChemistryDepartment- Education College of pure science – Basrah University. For potentiodynamic polarization studies, mild steel coupons with an exposed area of 2.0 cm^2 were used, and experiments were carried out in 100 cm^3 of solution containing different concentrations of inhibitor at 25 ^{o}C with the exposure time of 30 min (or until a steady-state open circuit potential was obtained). Tafel polarization obtained by changing the electrode potential automatically from (+250 mV to -250 mV) at open circuit potential with a scan rate 0.5 mV S^{-1} to study the effect of inhibitor on mild steel corrosion. The linear Tafel segment of cathodic and anodic curves were extrapolated to corrosion potential to obtain the corrosion current densities (I_{corr}).

2.5. Computation of Quantum Chemical Parameters

Quantum chemistry calculations were carried out by semi-empirical PM3 method from the program package Hyperchem version 7.52, 2002. A full optimization of all geometrical variables without any symmetry constraint was performed at the Restricted-Hartree-Fock (RHF) level. Molecular structures were optimized to the gradient <0.01 in the vacuum phase.

3. Result and discussion

3.1. Gravimetric measurements

3.1.1. Inhibition efficiency at different times

Inhibition efficiency *IE%*, surface coverage (θ) and corrosion rate $R_{corr.}$ were determined by using following equation:

$$IE\% = \left[\frac{W_{corr} - W_{corr(inh)}}{W_{corr}}\right] \times 100 \text{ - - - - - - } (1)$$

$$\theta = \frac{W_{corr} - W_{corr(inh)}}{W_{corr}} \text{ - - - - - - - - - - - - - - } (2)$$

where $W_{corr(inh)}$ and W_{corr} are the weight loss values in the presence and in the absence of inhibitor, respectively.

$$R_{corr.} = \frac{\Delta W * K}{A * D * t} \text{ - - - - - - - - - - - - - - - - } (3)$$

Where ΔW: weight losses of metal (gram), K: constant (5.34x10^5), A: sample area (cm^2), D: metal density (g/cm^3) and t: exposed time (hr).

Figure 1 shows the inhibition efficiencies (IE%) obtained from the weight loss measurements of C-steel for different concentrations of azo compound in 1M HCl 25^{o}C with different times of immersion. The results of weight loss measurements reported in the Table 1. These results show that by increasing the time the efficiency increases as a result of increased θ and there is good inhibition process for this azo compound where the efficiency in the range 87.5-91.9% at the best time of 4 hr. There is clear effect of inhibitor concentration on the efficiency, as shown in Table 1. For the second medium H_2SO_4, inhibition efficiency is less for HCl medium (81.7-85.2%) at time of 4 hr but this efficiency still represent a good behavior of this azo dye on the corrosion protection of C-steel, as shown in Figure 2 and Table 2.

Table 1: Effect of azo compound on the dissolution of C-steel in 1M HCl at different immersing time

Time (hr.)	1				2				3				4			
Conc. (M)	WL (gm)	Rcorr (mpy)	IE%	θ	WL (gm)	Rcorr (mpy)	IE%	θ	WL (gm)	Rcorr (mpy)	IE%	θ	WL (gm)	Rcorr (mpy)	IE%	θ
blank	0.0088	209.40			0.0253	301.01			0.0362	287.13			0.0699	415.83		
1x10^{-5}	0.003	71.39	65.91	0.6591	0.0062	73.77	75.49	0.7549	0.0075	59.49	79.28	0.7928	0.0087	51.76	87.55	0.8755
1x10^{-4}	0.0025	59.49	71.59	0.7159	0.0054	64.25	78.66	0.7866	0.0063	49.97	82.60	0.8260	0.0068	40.45	90.27	0.9027
1x10^{-3}	0.0021	49.97	76.14	0.7614	0.0042	49.97	83.40	0.8340	0.0054	42.83	85.08	0.8508	0.0056	33.31	91.99	0.9199

Table 2: Effect of azo compound on the dissolution of C-steel in 1M H2SO4 at different immersing time

Time (hr.)	1				2				3				4			
Conc. (M)	WL (gm)	Rcorr (mpy)	IE%	θ	WL (gm)	Rcorr (mpy)	IE%	θ	WL (gm)	Rcorr (mpy)	IE%	θ	WL (gm)	Rcorr (mpy)	IE%	θ
blank	0.0078	185.61			0.0211	251.04			0.0285	226.06			0.0399	237.36		
1x10^{-5}	0.0029	69.01	62.82	0.6282	0.006	71.39	71.56	0.7156	0.0071	56.32	75.09	0.7509	0.0073	43.43	81.70	0.8170
1x10^{-4}	0.0023	54.73	70.51	0.7051	0.0052	61.87	75.36	0.7536	0.0058	46.00	79.65	0.7965	0.0065	38.67	83.71	0.8371
1x10^{-3}	0.002	47.59	74.36	0.7436	0.0044	52.35	79.15	0.7915	0.0051	40.45	82.11	0.8211	0.0059	35.10	85.21	0.8521

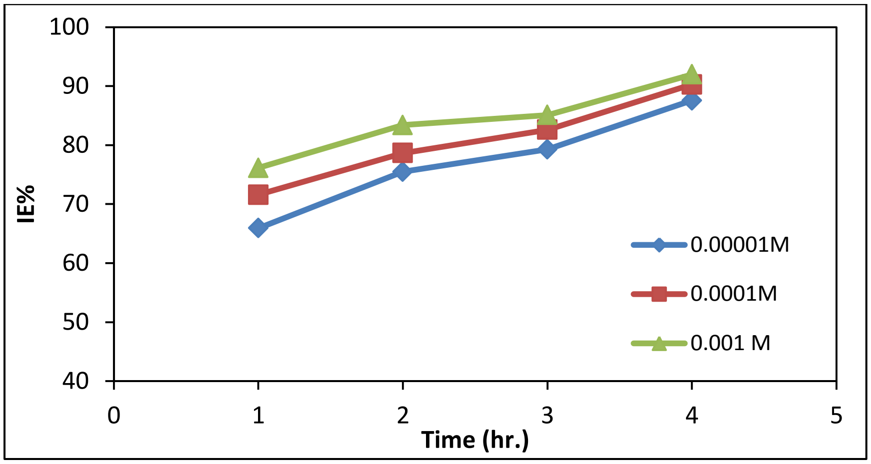

Figure 1: Inhibition efficiency IE% in HCl with time in the presence of different concentrations of azo at 25°C

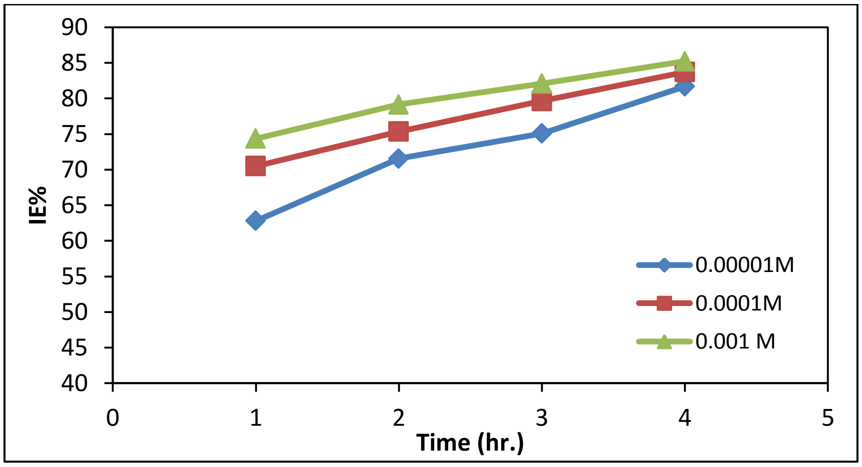

Figure 2: Inhibition efficiency IE% in 1M H_2SO_4 with time in the presence of different concentrations of azo at 25°C

3.1.2. Inhibition efficiency at different temperatures

Figures 3 and 4 show the inhibition efficiencies (IE %) obtained from the weight loss measurements of C-steel for different concentrations of azo compound in 1 M HCl and in 1M H_2SO_4, respectively, at 4 hr and at different temperatures. The results of weight loss measurements reported in the Tables 3 and 4. These results show that there is reversed proportional relationship between efficiency and temperature. It is clear that the rate of corrosion increases as the temperature increases. This indicates that the rising of temperature decreases the inhibition efficiency and the best inhibition efficiency is obtained at 25^{o}C.

Table 3: Effect of azo compound on the dissolution of C-steel in 1M HCl at different temperatures

Temp. (k)	**298**				**308**				**318**			
Conc. (M)	**WL (gm)**	**Rcorr (mpy)**	**IE%**	**θ**	**WL (gm)**	**Rcorr (mpy)**	**IE%**	**θ**	**WL (gm)**	**Rcorr (mpy)**	**IE%**	**θ**
blank	0.0699	415.82			0.0758	450.92			0.0969	576.44		
1x10^{-5}	0.0087	51.75	87.55	0.8755	0.0141	83.87	81.40	0.8140	0.0215	127.90	77.81	0.7781
1x10^{-4}	0.0068	40.45	90.27	0.9027	0.0109	64.84	85.62	0.8562	0.0187	111.24	80.70	0.8070
1x10^{-3}	0.0056	33.31	91.99	0.9199	0.0093	55.32	87.73	0.8773	0.0155	92.20	84.00	0.8400

Table 4: Effect of azo compound on the dissolution of C-steel in 1M H_2SO_4 at different temperatures

Temp. (k)	**298**				**308**				**318**			
Conc. (M)	**WL (gm)**	**Rcorr (mpy)**	**IE%**	**θ**	**WL (gm)**	**Rcorr (mpy)**	**IE%**	**θ**	**WL (gm)**	**Rcorr (mpy)**	**IE%**	**θ**
blank	0.0399	237.36			0.0472	280.79			0.0693	412.26		
1x10^{-5}	0.0073	43.43	81.70	0.8170	0.0103	61.27	78.18	0.7818	0.0172	102.32	75.18	0.7518
1x10^{-4}	0.0065	38.67	83.71	0.8371	0.0087	51.76	81.57	0.8157	0.0151	89.83	78.21	0.7821
1x10^{-3}	0.0059	35.10	85.21	0.8521	0.0079	47.00	83.26	0.8326	0.0138	82.09	80.09	0.8009

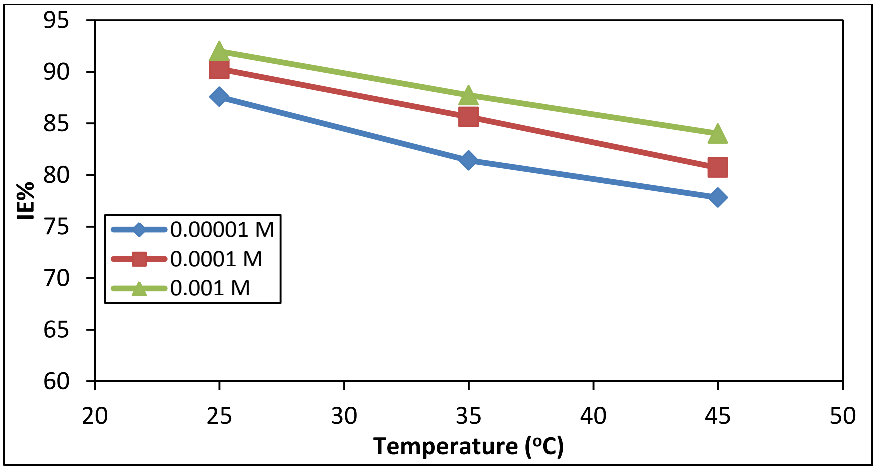

Figure 3: Inhibition efficiency IE% in HCl as a function of the temperature in the presence of different concentrations of azo dye at 4 hrs

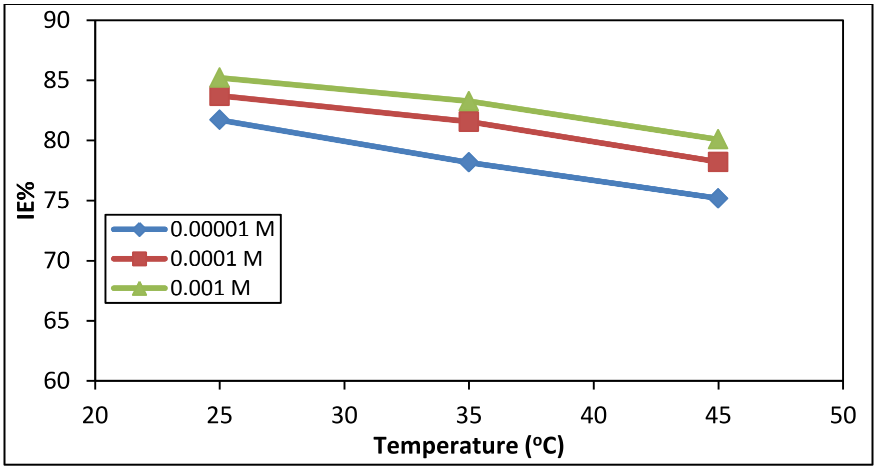

Figure 4: Inhibition Efficiency IE% in H_2SO_4 as a function of the temperature in the presence of different concentrations of azo dye at 4 hrs

3.2. Kinetic Parameters

In order to obtain the effect of inhibitors on the kinetic parameters, gravimetric weight loss experiments were conducted at 25, 35 and 45°C in 1M HCl or H_2SO_4 after 4 hr of immersion in the absence and presence of azo at $1x10^{-3}$M. The activation parameters for the system were calculated from Arrhenius-type plot (4) and transition state equation (5).

$$\log(R_{corr}) = \frac{-E_{act}}{2.303\,R\,T} + \log A \text{ - - - - - - (4)}$$

$$R_{corr} = \frac{RT}{Nh}\, exp\left(\frac{\Delta S}{R}\right)\, exp\left(-\frac{\Delta H}{RT}\right) \text{ - - - - - - (5)}$$

Figures 5 and 6 show Arrhenius plot (log R_{corr} vs. 1/T) for uninhibited carbon steel in 1 M HCl and in H_2SO_4, respectively and in presence of the studied azo compound. The values of E_a and Arrhenius factor can be obtained from the slope and the intercept of the straight lines, respectively and are given in Table 5. From the inspection of Table 5, it is clear that these values increase in the presence of the inhibitors. This was attributed to an appreciable decrease in the adsorption process of the inhibitor on the metal surface with increase of temperature and corresponding increase in the reaction rate because of the greater area of the metal that is exposed to acid solutions.

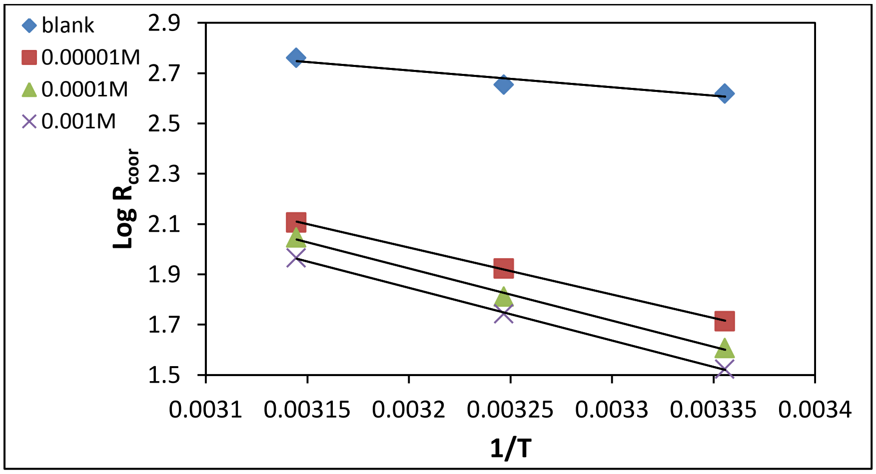

Figure 5: Arrhenius plots log $R_{corr.}$ versus 1/T at different concentration of azo dye in HCl

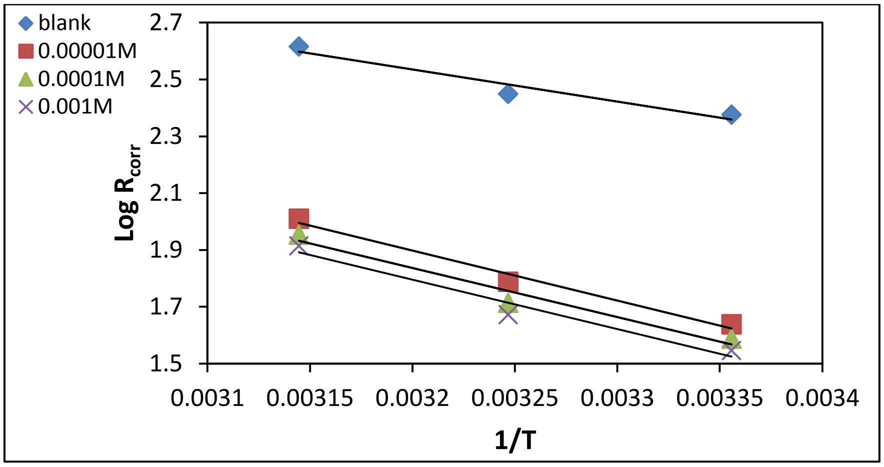

Figure 6: Arrhenius plots log $R_{corr.}$ versus 1/T at different concentration of azo dye in H_2SO_4

Table 5: Activation energy, Arrhenius factor, the enthalpy ΔH of activation and the entropy of activation of azo inhibitor

Conc. (M)	**in HCl**				**in H_2SO_4**			
	A	**E_a**	**ΔH**	**−ΔS**	**A**	**E_a**	**ΔH**	**−ΔS**
	$\times10^5$	**($kJmol^{-1}$)**			**$\times10^6$**	**($kJmol^{-1}$)**		
Blank	0.705	12.72	10.23	0.161	1.42	21.63	19.09	0.136
$1x10^{-5}$	923	35.68	33.09	0.101	33.7	33.67	31.11	0.109
$1x10^{-4}$	3780	39.81	37.24	0.089	23.2	33.08	30.52	0.113
$1x10^{-3}$	3520	40.02	37.53	0.090	23.4	33.35	30.79	0.112

Figures 7 and 8 show a plot of log (R_{corr}/T) against (1/T). Straight lines are obtained with a slope of (-ΔH/2.303R) and an intercept of (log R/Nh +-ΔS/2.303R) from which the values of ΔH and ΔS are calculated and listed in Table 5. From inspection of Table 5, it is clear that the positive values of ΔH reflect that the process of adsorption of the inhibitors on the metal surface is an endothermic process. The values of ΔS in the presence and absence of the inhibitors are negative. This implies that the activation complex is the rate determining step representing association rather than dissociation, indicating that a decrease in disorder takes place on going from reactant to the activated complex [13].

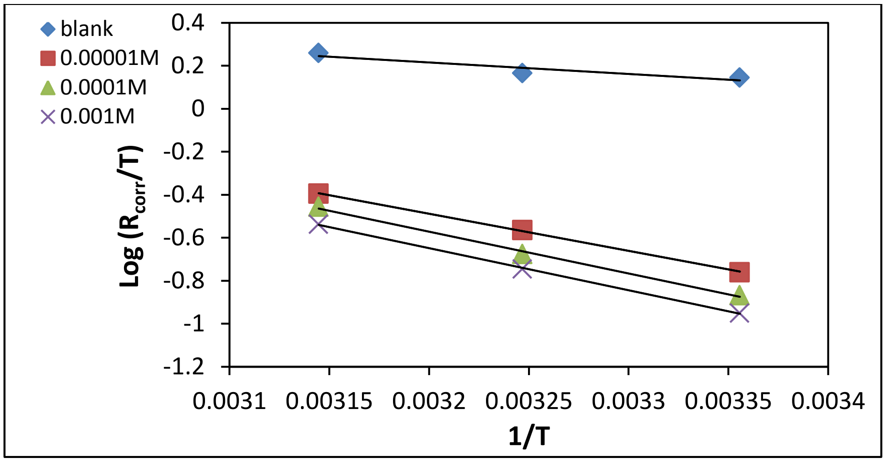

Figure 7: Arrhenius plots log ($R_{corr.}$/T) versus 1/T at different concentrations of azo dye in HCl

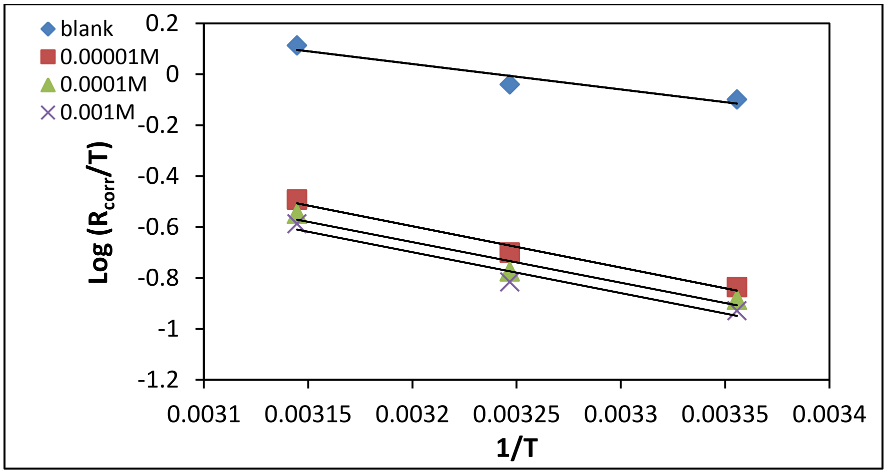

Figure 8 : Arrhenius plots log($R_{corr.}$/T) versus 1/T at different concentrations of azo dye in H_2SO_4

The relationship between the activation energy Ea and activation heat □H against the concentration of azo is shown in Figures 9 and 10. From the data obtained in Table 5, it seems that Ea and □H vary in the same manner. With an increase in concentration of azo dye, at first they increase, passing a maxima and thereafter remains approximately constant. This phenomenon is interpreted by the fact at a relative lower concentration around 10^{-5}M, the steel corrosion rate is chiefly decided by the kinetic parameters of activation[14].

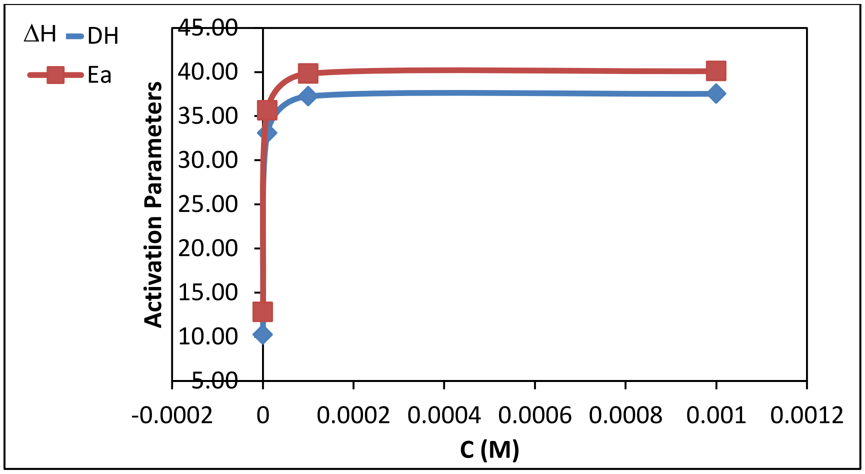

Figure 9: Variation of Ea and ΔH versus concentration of azo dye in HCl solution

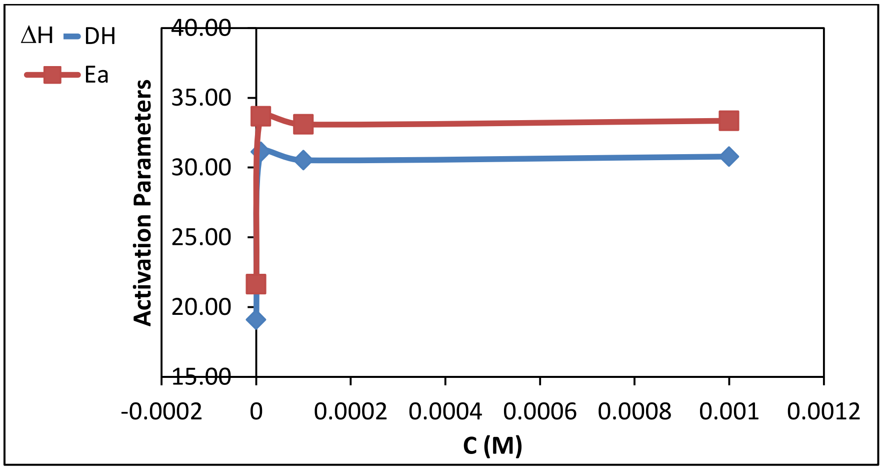

Figure 10: Variation of Ea and ΔH versus concentration of azo dye in H_2SO_4 solution

3.3. Adsorption Isotherm

Adsorption isotherms are very important in understanding the mechanism of inhibition of corrosion reaction. The most frequently used adsorption isotherms are Frundlich, Langmuir, Frumkin, and Temkin isotherms. The best fitted one follows Langmuir isotherm. Plotting (C/ θ) versus concentration (C) gives rise to straight lines, as shown in Figures 11 and 12. The obtained correlation coefficient R^2 is higher than 0.99 indicating that the principle inhibition action following Langmuir isotherm model [15], as shown by the following equation:

$$\frac{C}{\theta} = \frac{1}{K_{ads.}} + C \text{ - - - - - - - - - - - - - - - - (6)}$$

The large values of K_{ads} showed to strong adsorption process. The values of K_{ads} can be calculated from the intercepts of the straight lines of Figures 11 and 12, which have large values which indicated to strong adsorption process. The standard free energy of adsorption, ΔG_{ads} in kJ $mol^{-1}$of the azo dye is related to K_{ads} by the following equation:

$$K_{ads} = \frac{1}{55.5} \exp\left(\frac{-\Delta G^{o}_{ads}}{RT}\right) \text{ - - - - - - (7)}$$

where 55.5 is the concentration of water in the solution in mol/L, R is the universal gas constant in J mol^{-1}deg^{-1}, T is the absolute temperature.

The values of ΔG are found to be -41.28 , -43.88 and -44.19 kJ mol^{-1} for HCl solution, and -43.57, -43.95 and -45.38 kJ mol^{-1} for H_2SO_4 solution. Generally, if the values of ΔG lie in the range up to -20 kJ/mol, they are consistent with physisorption, due to electrostatic interaction between the charged inhibiting species and the charged metal, while those above -40 kJ/mol are associated with chemisorption as a result of sharing or transfer of electrons from inhibiting species to the metal surface to form a metal bond. The calculated ΔG_{ads} values in this study, Table 6, vary between -41.28 kJ/mol and -45.38 kJ/mol. These values indicate that the adsorption mechanism of all concentrations of the used inhibitor on metal in 1M HCl or H_2SO_4 solutions is through chemisorptions.

Table 6: Linear correlation coefficient R^2, equilibrium constant K and the free energy of adsorption ΔG_{ads} of azo dye in different solutions

Temp (K)	**in HCl**			**in H_2SO_4**		
	K (mol^{-1})	**-$\Delta G_{ads.}$ KJmol^{-1}**	**R^2**	**K (mol^{-1})**	**-$\Delta G_{ads.}$ KJmol^{-1}**	**R^2**
398	50000	41.28	0.9969	78265.63	43.57	0.9913
308	31034.7	43.88	0.9992	51429.75	43.95	0.9945
318	32727.87	44.19	0.9959	50421.1	45.38	0.9958

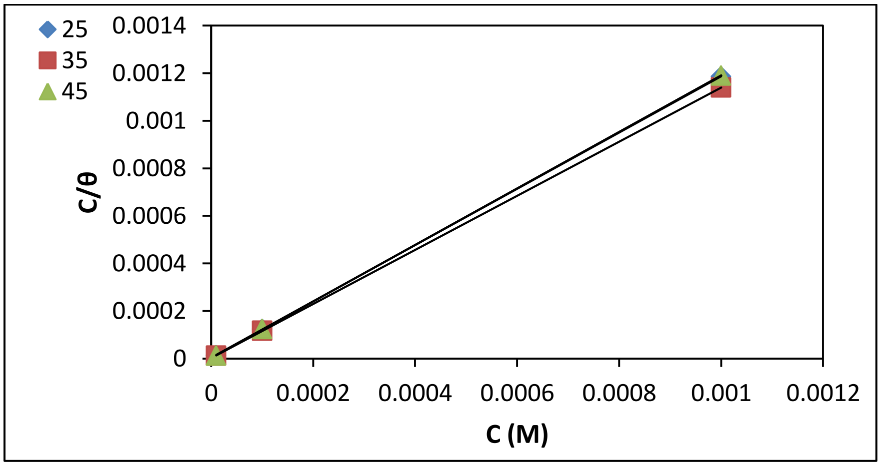

Figure 11: Langmuir adsorption isotherm of azo dye at different temperature in HCl solution

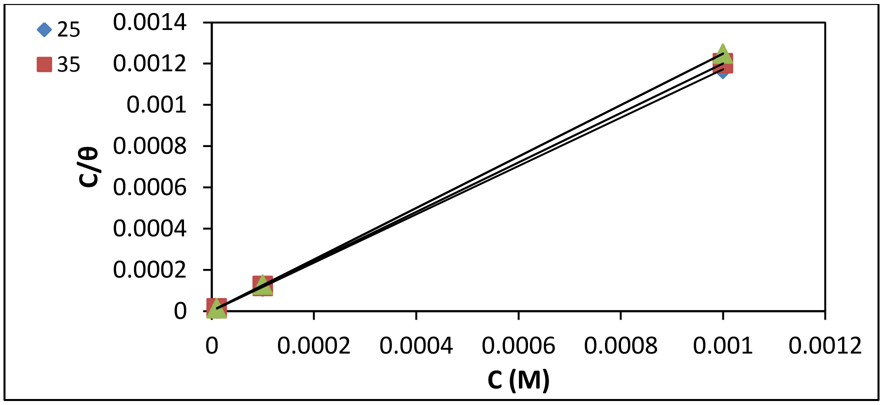

Figure 12: Langmuir adsorption isotherm of azo dye at different temperature in H_2SO_4 solution

3.4. Potentiodynamic polarization measurements

The inhibition efficiency was evaluated from the calculated I_{corr} values using the relationship:

$$E\% = \left[\frac{I_{corr} - I_{corr(inh)}}{I_{corr}}\right] \times 100 \text{ - - - - - - - - - - - } (8)$$

where I_{corr} and $I_{corr(inh)}$ are the corrosion current in the absence and in the presence of inhibitor, respectively.

The polarization curves of C-steel in 1 M HCl and H_2SO_4 with different concentrations of azo dye at 298 K are represented in Figures 13 and 14, respectively. It is clear that the inhibition increases as the azo dye concentration increases. It is evident from the Tafel plots that the inhibitor adsorption shifted the corrosion potential (E_{corr}) in the negative direction with reference to the blank in 1 M HCl or H_2SO_4, signifying that suppression of the cathodic reaction is the main effect of these corrosion inhibitors, Table 7.

Whereas, we found that by increasing the concentration, the current density decreases, which led to increase the corrosion efficiency. This may be attributed to decrease the adsorption process of inhibitor on the metal surface.

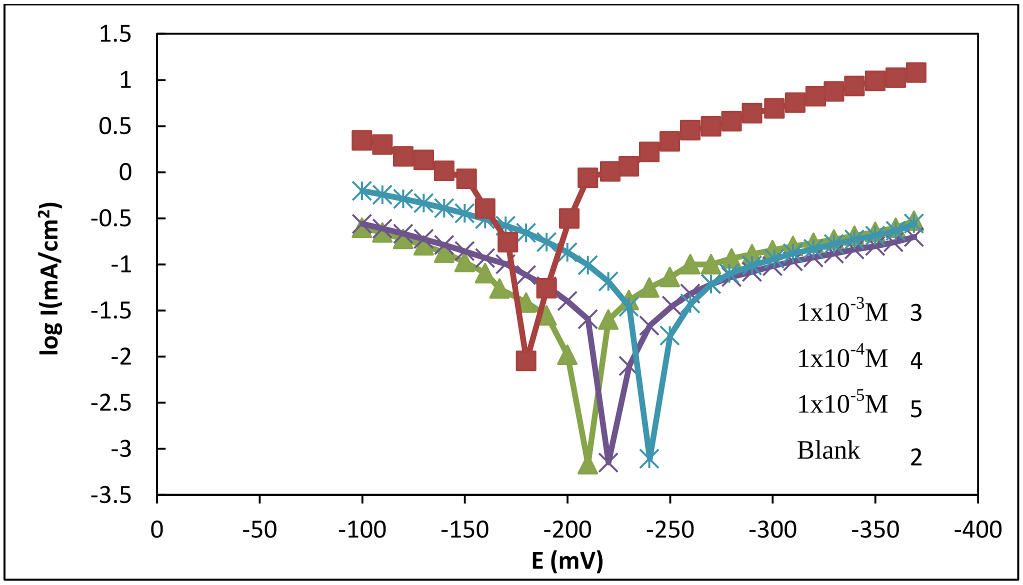

Figure 13: Anodic and cathodic polarization curves (Tafel curves) of mild steel in 1M HCl and in the absence and presence of different concentration of inhibitor at 25°C

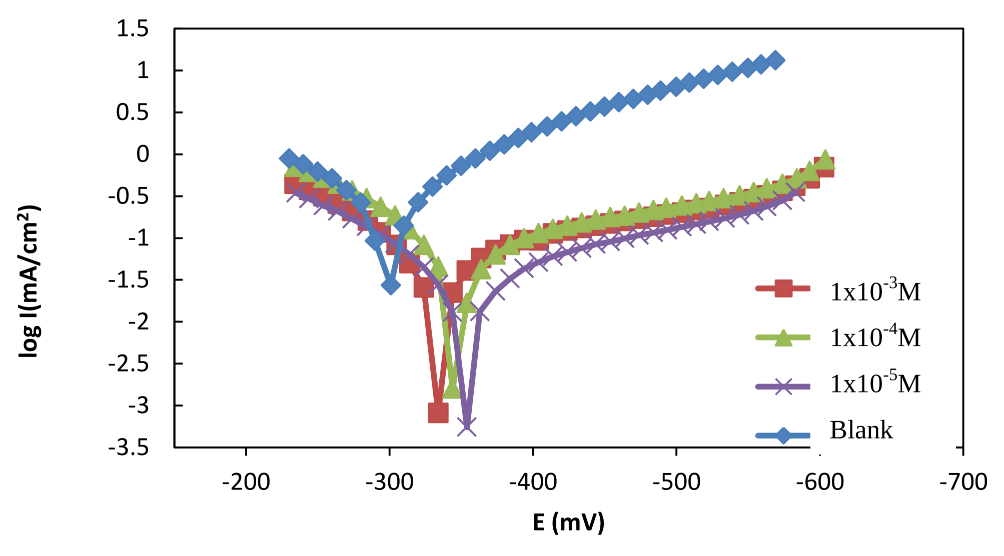

Figure 14: Anodic and cathodic polarization curves (Tafel curves) of mild steel in 1M HCl and in the absence and presence of different concentration of inhibitor at 25°C

Table 7: Electrochemical parameters for corrosion of mild steel in 1M HCl and H_2SO_4 in the presence of different concentration of inhibitor

Inhibitor Conc. (M)	Icorr. µA/cm2	Ecorr. mVolt	bC mV/dm	ba mV/dm	E%
In 1M HCl					
Blank	460.3	-185.3	-113.1	95.2	
$1x10^{-5}$	69.4	-249.9	-133.1	96	84.92
$1x10^{-4}$	46.5	-242.4	-151.9	94	89.89
$1x10^{-3}$	28.8	-225.4	-136.4	105.6	93.74
In 1M H_2SO_4					
Blank	734.7	-286.2	-113.6	115.9	
$1x10^{-5}$	137.4	-349.3	-174.5	88.8	81.29
$1x10^{-4}$	117.2	-343.4	-185.7	94.2	84.04
$1x10^{-3}$	97.4	-358.8	-128.8	99.6	86.74

3.5. Quantum Chemical Calculation

In order to study the effect of molecular structure on the inhibition efficiency, quantum chemical calculations were performed to use semi-empirical PM3 method. The optimized geometry of molecules is shown in Figure 8. The computed quantum chemical properties such as energy of highest occupied molecular orbital (E_{HOMO}), energy of lowest unoccupied molecular orbital (E_{LUMO}), the energy band gap (ΔE) and dipole moment (μ) are summarized in the Table 5.

Table 5: Calculated quantum chemical parameters of the azo dye compound

E_{HOMO} (eV)	E_{LUMO} (eV)	ΔE (eV)	μ (Debye)
-10.77	-5.3347	5.4353	3.962

E_{HOMO} often indicates the electron donating ability of the molecule and the inhibition efficiency increases with the increasing E_{HOMO} values. High E_{HOMO} values indicate that the molecule has a tendency to donate electrons to appropriate acceptor molecules with low energy empty molecular orbitals. The increasing values of the E_{HOMO} facilitate adsorption by influencing on the transport process through the adsorbed layer [16]. E_{LUMO} indicates the ability of the molecules to accept electrons. The lower value of E_{LUMO}, the more probable the molecule accepts electrons. The energy gap between *LUMO* and *HOMO* ($\Delta E = E_{LUMO} - E_{HOMO}$) is a parameter that the smaller value causes higher inhibition efficiencies of the molecule,[17] as shown in Figure 9. For the dipole moment (μ), higher values will favorite enhancement of corrosion inhibition [18]. It is reported that excellent corrosion inhibitors are usually those organic compounds which not only offer electrons to the unoccupied *d* orbital of the metal, but also accept free electrons from the metal into anti-bonding orbital to form a feedback bond [19].

It is clear from Table 5 that azo dye has the high values of E_{HOMO} , μ and the low values of E_{LUMO} *and* ΔE. These quantum chemical parameters indicate that this azo dye has high inhibition efficiency.

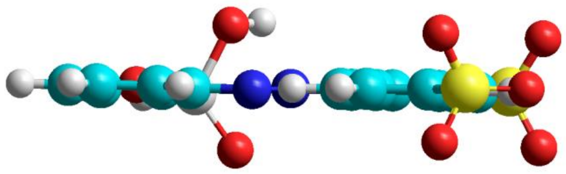

(a)

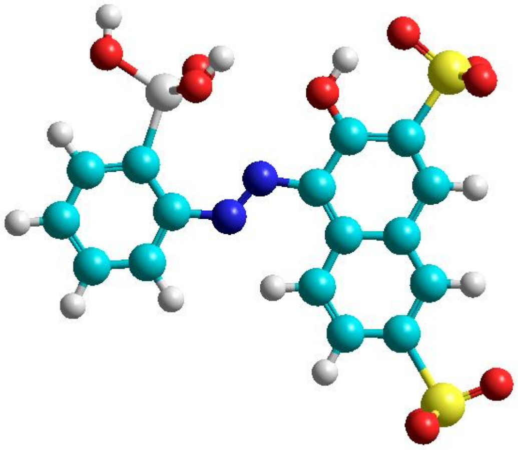

(b)

Figure 8: Optimized structures of thoron (a) is vertical view and (b) is plane view

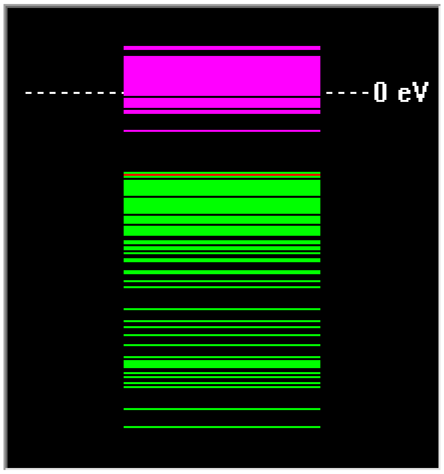

Figure 9: E_{HOMO} and E_{LUMO} energy levels of thoron compound

4. Conclusion

The corrosion behavior of C-steel in 1M HCl or 1M H_2SO_4 solution in the absence and presence of thoron compound was investigated using weight loss and galvanostatic polarization techniques. From the results obtained the following conclusions could be drawn:

1- The thoron exhibited good surface properties and inhibition efficiency reaches to 93.7%. The results show that its inhibition efficiencies in 1M HCl and 1M H_2SO_4 solutions increased with increase its concentration, but decreased with increase temperature.

2- The adsorption of azo dye compounds on the carbon steel surface at different temperature was found to obey the Langmuir adsorption isotherm. The adsorption process is a spontaneous and high value of equilibrium constants.

3- There are good agreements between weight loss and galvanostatic polarization techniques to determine the efficiency of corrosion inhibitor.

4- The quantum chemical calculations show that energy of highest occupied molecular orbital (E_{HOMO}), energy of lowest unoccupied molecular orbital (E_{LUMO}), the energy band gap (ΔE) and dipole moment (μ) are found to correlate well with experimental inhibition efficiencies of inhibitors.

References

[1] G. Avci, ***Mater. Chem. Phys.***, 112, 234 (2008).

[2] E. Bayol, T. Gürten, A. A. Gürten, and M. Erbil, ***Mater. Chem. Phys.,*** 112, 624 (2008).

[3] P. Lowmunkhong, D. Ungthararak and P. Sutthivaiyakit, ***Corr. Sci.***, 52, 30 (2010).

[4] H. H. Hassan, E. Abdelghani, and M. A. Amin,, ***Electrochim. Acta.,*** 52, 6359 (2007).

[5] E. Ispir, ***Dye Pigment***, 82, 13 (2009).

[6] H. Khanmohammadi and M. Darvishpour, ***J. Inorg. Organomet. Polym.,*** 21, 541 (2011).

[7] H. Dinc¸aple, F. Toker, I. Durucasu, N. Avcibas¸ and I. S. Icli, ***Dye Pigment***, 75, 11 (2007)

[8] S. Roy, T.N. Mandal, A.K. Barik, S. Pal, S. Gupta, A. Hazra, A.J. Butcher, A.D. Hunter, M. Zeller and S.K. Kar, ***Polyhedron***, 26, 2603 (2007)

[9] M. Odabas¸og˘lu, C¸ . Albayrak, R. O¨zkanca, F.Z. Aykan and P. Lonecke, ***J. Mol. Struct.***, 71, 840, (2007)

[10] D. Zhang, M. Zhang, Z. Liu, M. Yu, F. Li, T. Yi and C. Huang, ***Tetrahedron Lett.***, 47, 7093 (2006)

[11] P. Pattanyak, J.L. Pratihar, D. Patra, V.G. Puranik and S. Chatto-padhyay, ***Polyhedron***, 27, 2209 (2008)

[12] A. M. Ali, H. J. Mohammed and A. J. Khadhim, ***Islamic University J.***, 16, 85(2008).

[13] Salih S. Al-Juaid , ***Portugaliae Electrochimica Acta***, 25, 363 (2007).

[14] M. Bouklah, B. Hammouti, M. Lagrene and F. Bentiss, ***Corr. Sci.,*** 48, 2831(2006).

[15] E.E. Abd El Aal, S. Abd El Wanees, A. Farouk and S.M. Abd El Haleem, ***Corr. Sci.,*** 68, 14(2013).

[16] M. Behpour , S. M. Ghoreishi, N. Soltani, M. Salavati-Niasari, M. Hamadanian and A. Gandomi, ***Corr. Sci.,*** 50, 2172(2008).

[17] Y. M. Tang, W. Z. Yang, X. S. Yin, Y. Liu, R. Wan and J. T. Wang, ***Materials Chemistry and Physics,*** 116, 479(2009).

[18] M. Lebrini, M. Lagrenee, M. Traisnel, L. Gengembre, H. Vezin and F. Bentiss, ***Appl. Sur. Sci.***, Vol. 253, No. 23, 2007, 9267

[19] P. Zhao, Q. Liang and Y. Li, ***Appl. Sur. Sci.***, 252, 1596(2005).